ISSN 1936-878X/09/$36.00
PUBLISHED BY ELSEVIER INC.
DOI:10.1016/j.jcmg.2008.11.011

Molecular Imaging for Efficacy of Pharmacologic Intervention in Myocardial Remodeling

Susanne W. M. van den Borne, MD,*† Satoshi Isobe, MD, PHD,* H. Reinier Zandbergen, MD,† Peng Li, MD, PHD,* Artiom Petrov, PHD,* Nathan D. Wong, PHD, FACC,* Shinichiro Fujimoto, MD, PHD,* Ai Fujimoto, MD, PHD,* Dagfinn Lovhaug, PHD,‡ Jos F. M. Smits, PHD,† Mat J. A. P. Daemen, MD, PHD,† W. Matthijs Blankesteijn, PHD,† Chris Reutelingsperger, PHD,† Faiez Zannad, MD, PHD, FACC,§ Navneet Narula, MD,* Mani A. Vannan, MD, FACC,* Bertram Pitt, MD, FACC,¶ Leonard Hofstra, MD, PHD,† Jagat Narula, MD, PHD, FACC*

Irvine, California; Maastricht, the Netherlands; Oslo, Norway; Nancy, France; and Ann Arbor, Michigan

OBJECTIVES Using molecular imaging techniques, we examined interstitial alterations during postmyocardial infarction (MI) remodeling and assessed the efficacy of antiangiotensin and antimineralocorticoid intervention, alone and in combination.

BACKGROUND The antagonists of the renin-angiotensin-aldosterone axis restrict myocardial fibrosis and cardiac remodeling after MI and contribute to improved survival. Radionuclide imaging with technetium-99m–labeled Cy5.5 RGD imaging peptide (CRIP) targets myofibroblasts and indirectly allows monitoring of the extent of collagen deposition post-MI.

METHODS CRIP was intravenously administered for gamma imaging after 4 weeks of MI in 63 Swiss-Webster mice and in 6 unmanipulated mice. Of 63 animals, 50 were treated with captopril (C), losartan (L), spironolactone (S) alone, or in combination (CL, SC, SL, and SCL), 8 mice received no treatment. Echocardiography was performed for assessment of cardiac remodeling. Hearts were characterized histopathologically for the presence of myofibroblasts and thick and thin collagen fiber deposition.

RESULTS Acute MI size was similar in all groups. The quantitative CRIP percent injected dose per gram uptake was greatest in the infarct area of untreated control mice (2.30 $\pm$ 0.14%) and decreased significantly in animals treated with 1 agent (C, L, or S; 1.71 $\pm$ 0.35%; $p = 0.0002$). The addition of 2 (CL, SC, or SL 1.31 $\pm$ 0.40%; $p < 0.0001$) or 3 agents (SCL; 1.16 $\pm$ 0.26%; $p < 0.0001$) demonstrated further reduction in tracer uptake. The decrease in echocardiographic left ventricular function, strain and rotation parameters, as well as histologically verified deposition of thin collagen fibers, was significantly reduced in treatment groups and correlated with CRIP uptake.

CONCLUSIONS Radiolabeled CRIP allows for the evaluation of the efficacy of neurohumoral antagonists after MI and reconfirms superiority of combination therapy. If proven clinically, molecular imaging of the myocardial healing process may help plan an optimal treatment for patients susceptible to heart failure. (J Am Coll Cardiol Img 2009;2:187–98) © 2009 by the American College of Cardiology Foundation

From the *Division of Cardiology and Department of Pathology, University of California, Irvine School of Medicine, Irvine, California; †Department of Cardiology, Biochemistry, Pathology and Pharmacology, University Hospital Maastricht, Maastricht, the Netherlands; ‡GE Healthcare, AS, Oslo, Norway, §University Henri Poincaré, Nancy, France; and the ¶Division of Cardiology, University of Michigan, Ann Arbor, Michigan. Dr. van den Borne was partially supported by a grant from the Netherlands Heart Foundation (2006R013). Dr. Lovhaug is an employee of GE Healthcare, involved in tracer preparation for the imaging studies. Dr. Pitt is a consultant to Pfizer, Merck, Takeda, Astra Zeneca, Synvista, Novartis, and Nile therapeutics but has no conflicts directly with the project. H. William Strauss, MD, acted as Guest Editor for this paper.

Manuscript received June 9, 2008; revised manuscript received October 31, 2008, accepted November 6, 2008.

JACC: CARDIOVASCULAR IMAGING, VOL. 2, NO. 2, 2009
FEBRUARY 2009:187–98

Up regulation of the renin-angiotensin-aldosterone axis after myocardial infarction (MI) contributes to the process of cardiac remodeling and hence the evolution of heart failure (1–4). Although this remodeling process is initiated by myocyte loss, interstitial and myocytic alterations continue to occur inexorably even after the initial injury has abated (5–7). Anti-angiotensin (8–10) and antialdosterone (11) treatments effectively control this process and delay or prevent the development of heart failure (12–15).

See page 199

These therapeutic interventions reduce the extent of interstitial collagen deposition, which is considered to be the basis of their efficacy (1,2). The combination of these agents has been shown to be more effective than the solitary agents (16,17).

The efficacy of pharmacologic intervention in a clinical milieu is variable, and it is desirable to define optimal use of antiremodeling agents for individual patients. Although pharmacogenomics has been proposed as an important determinant of such a strategy (18,19), the role of phenotypic characterization by novel imaging methods is also being explored (4). It has recently been reported that the extent of new collagen deposition can be assessed by molecular imaging employing technetium-99m-labeled Cy5.5-RGD-imaging peptide (^{99m}Tc-CRIP) (20). Through Arg-Gly-Asp (RGD)-based targeting, ^{99m}Tc-CRIP binds to the myofibroblasts in the healing infarct and correlates with the extent of new collagen deposition after experimental MI (20). In our preliminary experiment we proposed that such imaging strategy may have a role in identifying the impact of a therapeutic intervention on collagen deposition and hence the efficacy of therapy. In the present study, we evaluated the effect of an angiotensin-converting enzyme inhibitor (ACE-I), an angiotensin receptor blocker (ARB), and a selective aldosterone receptor antagonist (SARA), individually and in combination, on infarct healing by using ^{99m}Tc-CRIP imaging.

ABBREVIATIONS AND ACRONYMS

ACE-I = angiotensin-converting enzyme inhibitor

ARB = angiotensin receptor blocker

ASMA = alpha smooth muscle actin

C = captopril

CRIP = Cy5.5-RGD imaging peptide

L = losartan

LV = left ventricular

MI = myocardial infarction

RGD = Arg-Gly-Asp.

S = spironolactone

SARA = selective aldosterone receptor antagonist

sCRIP = scrambled Cy5.5-RGD imaging peptide

^{99m}Tc = technetium-99m

METHODS

Study protocol. The present study was performed in 69 Swiss-Webster mice. Of these, MI was produced in 63 mice by occlusion of the left coronary artery. Echocardiograms were obtained before and after coronary occlusion to demonstrate the basal left ventricular (LV) dimensions and function in addition to the infarct size. Of the 63 infarcted mice, 20 mice received a single agent intervention (1Rx); 8, 6, and 6 animals were started on spironolactone (S), captopril (C), and losartan (L), respectively. A total of 22 of 63 animals received dual therapy (2Rx); 6, 8, and 8 animals were started on a combination of captopril + losartan (CL), spironolactone + captopril (SC), or spironolactone + losartan (SL), respectively, and 8 of 63 post-MI animals received a combination of 3 neurohumoral antagonists (3Rx, spironolactone + captopril + losartan [SCL]) (Table 1). Eight post-MI animals did not receive any pharmacologic agent and served as treatment controls (No Rx), and 5 post-MI animals received a scrambled version of the imaging peptide (sCRIP) to serve as tracer controls. In addition to 63 infarcted mice, 6 unmanipulated animals were included in the imaging protocol as disease control animals. After 4 weeks, all animals again underwent echocardiographic examination for the characterization of the remodeling process and received ^{99m}Tc-labeled CRIP intravenously. After 3.5 h of CRIP administration, hearts were explanted and ex vivo imaging was performed with a microSPECT camera. The hearts were then sectioned into 3 cross-sectional bread-loaf slices to represent apical (predominantly infarct), middle, and the basal (predominantly remote) areas. All samples were gamma-counted for quantitative ^{99m}Tc-CRIP (and sCRIP) uptake. Subsequently, all myocardial specimens were processed for histopathological characterization, particularly the extent of myofibroblast proliferation and thick and thin collagen fiber deposition.

Experimental MI in mice. This experimental protocol was approved by the Institutional Animal Care and Use Committee of the University of California Irvine School of Medicine. In 63 adult Swiss Webster male mice (age, 3 months; body weight, ~50 g), the lateral branch of the left coronary artery was ligated under pentobarbital (75 mg/kg intraperitoneally) and gas anesthesia (2.0 to 3.0% isoflurane) to induce MI, as per previous description (21). Successful ligation was verified by visual inspection of myocardial blanching and akinesis or dyskinesis of the apical segment. The chest was closed, and animals were gradually weaned from the respirator. Six of the 69 mice were left unmanipulated as

Table 1. Various Treatment Groups, Dosage Schedules, and Quantitative CRIP Uptake

	Dose				Infarct		Remote	
Group	Spironolactone	Captopril	Losartan	n	%ID/g	p Value	%ID/g	p Value
Control	—	—	—	6	0.590 ± 0.19	†	0.677 ± 0.162	NS
No Rx	—	—	—	8	2.302 ± 0.136	*	0.921 ± 0.218	NS
S	20 mg/kg/day	—	—	8	1.798 ± 0.437	*†	0.903 ± 0.221	NS
C	—	60 mg/kg/day	—	6	1.718 ± 0.296	*†	0.867 ± 0.234	NS
L	—	—	20 mg/kg/day	6	1.576 ± 0.279	*†	0.752 ± 0.114	NS
CL	—	30 mg/kg/day	10 mg/kg/day	6	1.374 ± 0.549	*†	0.783 ± 0.272	NS
SC	20 mg/kg/day	60 mg/kg/day	—	8	1.280 ± 0.408	*†	0.786 ± 0.168	NS
SL	20 mg/kg/day	—	20 mg/kg/day	8	1.293 ± 0.316	*†	0.821 ± 0.364	NS
SCL	20 mg/kg/day	60 mg/kg/day	20 mg/kg/day	8	1.157 ± 0.261	*†	0.796 ± 0.196	NS

The quantitative CRIP uptake in control animals was obtained from the myocardial specimen corresponding to infarct and remote regions of post-MI animals. *$p < 0.05$ to < 0.0001 compared with control animals. †$p < 0.05$ to < 0.0001 compared with No Rx-treated animals.
99mTc-CRP = technetium-99m-labeled Cy5.5-RGD imaging peptide; MI = myocardial infarction; NS = nonsignificant.

disease control mice for comparison with the post-MI mice.

Treatment protocols after MI in mice. Captopril (Sigma, St. Louis, Missouri) and losartan (kind gift of Merck, Rahway, New Jersey) were administered in the drinking water, 60 and 20 mg/kg/day, respectively. Spironolactone (Innovative Research of America, Sarasota, Florida) was administered via a subcutaneous pellet, releasing 1 mg/day, placed under the skin on the back immediately after MI surgery. The animals received the intervention for 4 weeks beginning immediately after surgery (Table 1).

Echocardiography. Echocardiographic studies were performed in all mice for the evaluation of left ventricular dimensions and function, as reported previously (20). All animals underwent 3 echocardiographic studies; one performed at baseline level, one immediately after MI, and one 4 weeks after MI, just before CRIP imaging. Mice were anesthetized with 2% isoflurane, and echocardiograms were made (Sequoia, Siemens, Mountain View, California) with a 14-MHz linear probe (15L8, Acuson). An advanced high frame rate imaging technique (Paragon, Siemens) was adopted to increase temporal resolution at a frame rate of 120 fps. B-mode images of LV parasternal long-axis, parasternal short-axis, and apical views were digitally acquired at 2 to 3 cardiac cycle lengths. Images of LV short-axis were standardized at 3 levels: base, mid, and apex. M-mode imaging was unified according to the American Society of Echocardiography guidelines for measurements of wall thickness, chamber dimensions, and functional parameters (22). Infarction area and LV area were measured by tracing relative endocardial borders respectively on the long-axis images. Myocardial infarction percentage was calculated as: infarction area/LV area × 100. Left ventricular cavity dimensions, ejection fraction, strain, and rotation were calculated (23).

Radionuclide imaging with ^{99m}Tc-CRIP. The technetium-99m-labeled Cy5.5-RGD imaging peptide (AH110863, kind gift of GE Healthcare, Oslo, Norway) is a 2.5-kDa peptide conjugated to both a fluorescent cyanine dye Cy5.5 and the chelating agent cPN216, which is linked for radiolabeling of the peptide with ^{99m}Tc. The peptide comprises 10 amino acids, contains an RGD motif, and has a bicyclic structure formed by a disulfide and a thioether bridge. The dye moiety and the chelating agent are conjugated to the peptide by the side-chains of lysine residues at the N- and C-terminal ends, respectively. The technetium-99m–labeled Cy5.5-RGD imaging peptide, by RGD-based targeting, binds to myofibroblasts (20) and is labeled with ^{99m}Tc for radionuclide imaging. For radiolabeling, 50 μg of ^{99m}Tc-CRIP was dissolved in 50 μl of methanol and then added to the freeze-dried kit. A total of 1.0 ml of $^{99m}TcO_4^-$ was added to the compound and left at room temperature for 20 to 30 min. Instant thin-layer chromatography confirmed radiopurity of more than 90%. Then, 3.7 ± 0.2 mCi (137 ± 7.4 MBq) of ^{99m}Tc-CRIP was injected intravenously through the tail vein. At 3.5 h after ^{99m}Tc-CRIP administration, mice were sacrificed with an overdose of pentobarbital (150 mg/kg intraperitoneally). Hearts were carefully dissected and planar images of ex vivo hearts were acquired for 15 min in 128 × 128 matrix with the use of a low-energy, high-resolution pinhole collimator, mounted in a dual-head micro single-photon emission computed tomography gamma camera (X-SPECT, Gamma Medica, Inc., Northridge, California). Thereafter, hearts were cut into apical, middle, and basal slices.

The quantitative CRIP uptake was determined with a gamma scintillation counter (1480 Wizard 3″, Wallace & Co., Monrovia, California). We also determined CRIP biodistribution and radiation burden to lung, liver, spleen, and kidney.

Histological evaluation of myocardial specimens. After completion of the nuclear studies, the 3 bread-loaf slices were washed in phosphate-buffered saline, fixed in 4% paraformaldehyde in phosphate-buffered saline for 24 h, processed, and embedded in paraffin; then, 4-μm sections were prepared. After deparaffinization and rehydration, sections were stained with hematoxylin & eosin, Masson's trichrome, and picro-Sirius red, as reported previously (20). In picro-Sirius–stained sections, the relative collagen areas in the infarcted, and remote areas were determined under a microscope (×200) coupled to a computerized morphometry system (Quantimet, Leica, Cambridge, United Kingdom). The quality of collagen fibers was investigated with the use of Sirius red polarization microscopy, allowing quantitation of the thick, tightly packed, more mature orange/red fibers and the newly formed, thin, loosely assembled yellow/green fibers (24,25). Approximately 4 to 5 fields per section were analyzed in the myocardium. Finally, alpha smooth muscle actin (ASMA) was used to determine myofibroblasts in the infarct area, as reported earlier (20). Alpha smooth muscle actin area was quantified by Quantimet analysis in 4 to 5 fields per section; ASMA uptake was only counted for myofibroblasts, and care was taken not to include ASMA uptake observed in vasculature.

Statistical analysis. Quantitative radiotracer uptake was calculated as percent total injected dose per gram (%ID/g) of the tissue. Radiotracer uptake and echocardiographic measurements were expressed as mean ± standard deviation. In our previous study (20), CRIP uptake was reduced by >25% in the captopril group compared with the untreated group and in combination treatment (losartan plus captopril) compared with single therapy (captopril alone) group; as such, we propose that having at least 6 mice per group is sufficient to detect, with at least 90% power and alpha = 0.01, reductions in the uptake of CRIP of at least 25% in treated compared with untreated animals, or 2 versus 1 agent groups. This calculation confirms that our current study is well-powered. To determine the statistical significance of differences among treatment groups, we used 1-way analysis of variance followed by post-hoc analysis for multiple comparisons. Because we had a limited number of pre-specified pairwise comparisons, namely comparison of control and untreated animals with uptake among 1, 2, or 3 Rx-treated animals, we used the Bonferroni's method for post-hoc analysis. The correlation between the quantitative tracer uptake and echocardiographic parameters or histological characteristics was evaluated by linear regression analysis. p Values < 0.05 were considered as statistically significant.

RESULTS

Uptake of ^{99m}Tc-CRIP and pharmacologic intervention. Maximum CRIP uptake was observed in the infarct zone of the untreated post-MI mice; CRIP uptake was substantially reduced in the treated animals (Table 1, Fig. 1A); no CRIP uptake was observed in the unmanipulated hearts. Scrambled CRIP, which has a deranged RGD sequence, did not show uptake in the infarcted myocardium and demonstrated that CRIP uptake is RGD dependent and specific.

The quantitative CRIP uptake in the myocardial tissue specimens was calculated and represented as percent of injected CRIP dose per gram (%ID/g) of myocardial tissue. We observed CRIP uptake in the infarcted area to be the greatest in the untreated MI group (No Rx; 2.30 ± 0.14%). There was a significant reduction in CRIP uptake in the infarct area in all treated animals (1.46 ± 0.42%) compared with the untreated animals ($p < 0.0001$). The reduction of uptake was significant even when the animals were treated with a single neurohumoral antagonist (1Rx, 1.71 ± 0.35%, $p = 0.0002$) (Fig 1B). Each agent was independently effective; spironolactone (1.80 ± 0.44%; $p = 0.0011$), captopril (1.72 ± 0.30%; $p = 0.0059$), and losartan (1.58 ± 0.28%; $p < 0.0001$) (Table 1).

The use of 2 neurohumoral antagonists (2Rx, 1.31 ± 0.40%) influenced the CRIP uptake to a greater extent than a single agent (1Rx, 1.71 ± 0.35%) treatment ($p = 0.0005$) (Fig 1B). Uptake with various combinations was as follows; CL (1.37 ± 0.55%; $p < 0.0001$), SC (1.28 ± 0.41%; $p < 0.0001$), and SL (1.29 ± 0.32%; $p<0.0001$) (Table 1). The combination of all 3 agents further reduced the CRIP uptake (3Rx, 1.16 ± 0.26%) in the infarct area (Fig. 1B). The decrease in CRIP uptake in triple-treated animals was significantly lower than 1-agent treatment ($p = 0.0001$) but was statistically insignificantly reduced compared with 2-agent therapy ($p = 0.33$) (Fig. 1).

We found that CRIP uptake in the remote myocardium tended to be increased, although not

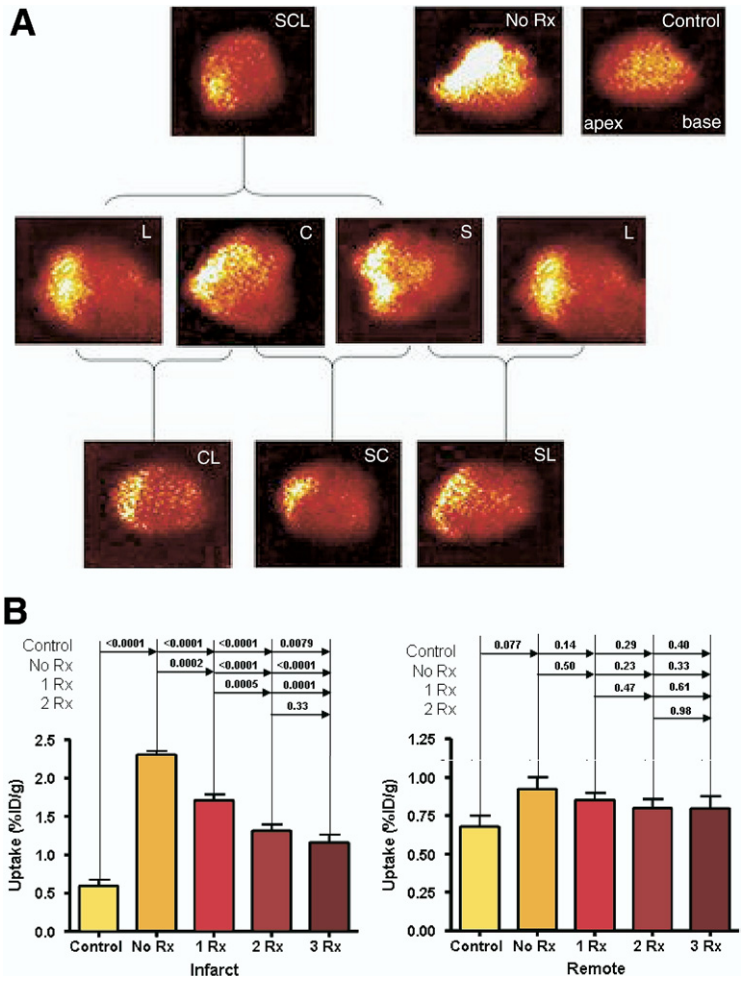

Figure 1. Radiolabeled CRIP Uptake After Neurohumoral Antagonist Treatment in Post-MI Animals

(A) Disease control (unmanipulated) heart with RGD probe shows no radiotracer uptake in ex vivo image of the heart. However, intense ^{99m}Tc-CRIP uptake is found in 4-week untreated (no Rx) post-MI animals **(upper panel, right)**. The uptake in the infarcted area is reduced after neurohumoral treatment with solitary agents and combination therapy **(middle and lower panels)**. Losartan (L) images are displayed twice **(middle panel)** for the convenience of comparison. C = captopril; S = spironolactone. **(B)** Quantitative ^{99m}Tc-CRIP uptake in the infarct (apex, **above**) and remote (base, **below**) areas. The %ID/g uptake in the infarct area is greatest in untreated mice, followed by treatment with 1 (1Rx), 2 (2Rx), and 3 (3Rx) agents, respectively. On the other hand, the uptake in the remote area shows no significant differences between treated and untreated animals. Quantitative data confirmed the findings of ex vivo images. Data are presented as mean ± SEM. ^{99m}Tc-CRIP = technetium-99m-labeled Cy5.5-RGD imaging peptide; MI = myocardial infarction; %ID/g = percent of injected CRIP dose per gram; RGD = Arg-Gly-Asp.

statistically significant, in the untreated post-MI animals (0.92 ± 0.22) compared with the unmanipulated control animals with no infarcts (0.68 ± 0.16, p = 0.077) (Fig. 1B).

Echocardiographic examination and remodeling characteristics. As shown in Table 2, initial MI size was similar in all animal groups. During the 4-week follow-up period, there was a reduction in LV ejection fraction in untreated post-MI (30 ± 8%) animals compared with unmanipulated disease control animals (64 ± 4%, p < 0.0001). Neurohumoral antagonists significantly prevented the functional loss (ejection fraction 44 ± 10%), compared with untreated animals (30 ± 8%; p = 0.0016). Similar to LV ejection fraction, there was a significant decrease in the myocardial strain development in untreated animals (−4.59 ± 1.85 U %) compared with unmanipulated (−12.00 ± 2.31 U %) animals (p < 0.0001); loss of myocardial strain was significantly prevented by treatment with neurohumoral agents (−8.04 ± 2.4 U %, p = 0.0005). The strain development in 1Rx (−7.17 ± 2.28 U %, p = 0.0126), 2Rx (−8.28 ± 2.51 U %, p = 0.0011), and 3Rx

Table 2. Echocardiographic Observations in Control, Untreated, and Treated Animal Groups

		Control	no RX	S	C	L	CL	SC	SL	SCL
n		6	8	8	6	6	6	8	8	8
Day 0	BW (g)	46 ± 3	45 ± 9	53 ± 5	46 ± 6	53 ± 8	42 ± 4	48 ± 6	47 ± 4	48 ± 6
	MI (%)	0	41 ± 6*	41 ± 9*	39 ± 6*	42 ± 16*	40 ± 5*	40 ± 8*	41 ± 9*	43 ± 9*
4 weeks	LVIDd (cm)	0.46 ± 0.02	0.55 ± 0.08*	0.52 ± 0.08*	0.52 ± 0.06*	0.50 ± 0.05	0.5 ± 0.06	0.52 ± 0.05	0.51 ± 0.06	0.50 ± 0.03
	LVIDs (cm)	0.30 ± 0.01	0.46 ± 0.10*	0.46 ± 0.11*	0.41 ± 0.08*	0.41 ± 0.06*	0.40 ± 0.10*	0.43 ± 0.09*	0.43 ± 0.07*	0.44 ± 0.07*
	EF (%)	64 ± 4	30 ± 8*	39 ± 10*	43 ± 6*†	47 ± 9*†	44 ± 14*†	43 ± 12*†	47 ± 14*†	44 ± 9*†
	Strain (unit %)	−12.0 ± C122.3	−4.6 ± 1.9*	−6.9 ± 2.6*	−7.7 ± 1.6*†	−7.0 ± 2.7*	−7.3 ± 03.1*†	−8.0 ± 1.6*†	−9.1 ± 2.8*†‡	−9.3 ± 1.7*†‡
	Rotation (°)	1.85 ± 0.14	0.22 ± 0.11*	0.48 ± 0.21*†	0.50 ± 0.10*†	0.50 ± 0.20*†	0.53 ± 0.21*†	0.54 ± 0.15*†	0.62 ± 0.21*†	0.63 ± 0.17*†

*$p < 0.05$ to < 0.0001 compared with control mice. †$p < 0.05$ to < 0.001 compared with untreated mice (no Rx). ‡$p < 0.05$ compared with spironolactone.
BW = body weight; C = captopril; CL = captopril and losartan; EF = ejection fraction; L = losartan; LVIDd = left ventricular diastolic dimension; LVIDs = left ventricular systolic dimension; MI = myocardial infarction; S = spironolactone; SC = spironolactone and captopril; SCL = spironolactone, captopril, and losatran; SL = spironolactone and losartan.

(−9.33 ± 1.7 U %, $p < 0.0001$) groups was better preserved compared with the untreated control group. However, the preservation of strain development did not reach statistical significance on comparison of 1Rx versus 2Rx ($p = 0.13$) or 2Rx versus 3Rx ($p = 0.25$) agents; 3Rx was statistically significantly better than the 1Rx intervention ($p = 0.0168$). The results of loss of apical rotation or counterclockwise twist of the LV were similar to the loss of strain development. The rotation in all (0.55 ± 0.18°, $p < 0.0001$), 1Rx (0.49 ± 0.17°, $p = 0.0006$), 2Rx (0.57 ± 0.19°, $p < 0.0001$), and 3Rx (0.63 ± 0.17°, $p < 0.0001$) groups was preserved compared with the untreated control group. However, once again, the prevention of rotational loss did not reach statistical significance on comparison of 1Rx versus 2Rx ($p = 0.17$) or 2Rx versus 3Rx ($p = 0.36$) agents; 3Rx was statistically significantly better than the 1Rx intervention ($p = 0.048$). The LV ejection fraction, strain development, and rotation correlated with %ID/g CRIP uptake ($r^2 = 0.309$, $= 0.397$, and $= 0.469$, and $p < 0.0001$, < 0.0001, and < 0.0001, respectively) (Fig. 2).

Histologic characterization of infarct and remote myocardium and correlation with ^{99m}Tc-CRIP uptake. Masson's trichrome and picro Sirius red staining (Fig. 3) of the myocardial slices allowed the assessment of total collagen content and the composition in thick and thin collagen fibers. The percent collagen content in the infarcted area in untreated animals was 79 ± 4%, which reduced substantially in the treated animals (66 ± 8%, $p < 0.0001$) (Fig. 4A, Table 3). The collagen content decreased in animals treated with 1Rx (71 ± 7%, $p = 0.006$), 2Rx (64 ± 9%, $p < 0.0001$), or 3Rx (65 ± 4%, $p = 0.0008$) agents (Fig 4A). The results were similar for the yellow-green collagen fiber deposition in the infarcted myocardium, suggesting a decrease in new or thin collagen fiber synthesis (Fig. 4C). The new, thin collagen fibers correlated with CRIP uptake in the infarct ($r^2 = 0.5475$, $p < 0.0001$) (Fig. 4E). In the remote region, the overall collagen deposition was markedly lower compared with the infarct region. The collagen content of the untreated remote myocardium (No Rx, 2.1 ± 0.6%) was significantly greater than the unmanipulated hearts (0.73 ± 0.2%, $p < 0.0001$) (Fig 4B). A marked decrease in collagen content and yellow-green collagen fiber deposition was observed in the remote region after treatment (Fig. 4D, Table 3); collagen content in treated animals was not different from unmanipulated animals. There was a direct correlation between tracer uptake and thin collagen fiber deposition in the remote region ($r^2 = 0.347$; $p < 0.0001$) (Fig. 4F).

We performed ASMA staining for quantitation of the myofibroblasts (Fig. 5A). The ASMA-positive area was substantially larger in the untreated animals (No Rx, 6.11 ± 5.17μm^2) compared with the unmanipulated animals (0.007 ± 0.01μm^2, $p = 0.013$). Treatment with 1Rx (4.91 ± 2.12 μm^2, $p = 0.51$), 2Rx (2.22 ± 3.30 μm^2, $p = 0.037$), or 3Rx (1.54 ± 0.92 μm^2, $p = 0.039$) interventions substantially restricted the myofibroblast prevalence (Fig. 5B, Table 3). There was a directly proportional relationship between CRIP uptake and ASMA-positive area ($r^2 = 0.582$, $p < 0.0001$) (Fig. 5C).

DISCUSSION

Molecular imaging in myocardial remodeling. The present study used molecular imaging of myofibroblasts during infarct healing. The radiotracer, CRIP, contains an RGD sequence and binds to myofibroblasts through activated $\alpha v\beta 3/5$ inte-

grins with an affinity of 1 to 3 nmol/l (20); RGD is also known to commonly target the integrin expression associated with neoangiogenesis early after MI and macrophage influx during infarct healing. We have observed that after 2 weeks of infarct healing, myofibroblasts comprise a predominant target for RGD probes (20). In addition, a specific noncovalent interaction of CRIP also was observed with custom-made DDX-sequence contained within pro-collagen I. The previous study using ^{99m}Tc-CRIP had demonstrated the feasibility of noninvasively imaging the extent of myofibroblasts prevalence in a post-MI mouse model (20). The CRIP uptake receded over time in the infarct region with substantial resolution over the course of 3 months after the myocardial injury. This previous report also demonstrated that the uptake was significantly reduced at 4 weeks upon treatment with captopril alone or in combination with losartan and proposed that CRIP uptake could monitor the efficacy of neurohumoral antagonists and help identify the optimum level of therapeutic intervention (20). A simultaneously conducted clinical study, using RGD-seeking peptide demonstrated the feasibility of molecular imaging early after MI (26). The radiotracer uptake after MI predicted the extent of eventual magnetic resonance imaging-verified fibrosis after 1 year. On the basis of these results, the present study investigated the effect of various neurohumoral antagonists, alone or in combination, on the extent of myocardial interstitial alterations in a 4-week post-MI mouse model.

This study confirmed the efficacy of antiangiotensin and antialdosterone intervention on interstitial alterations and demonstrated that combination of 2 neurohumoral antagonists was superior to an individual agent; 3 agents decreased the radiotracer uptake further, albeit not significantly. The radiotracer uptake correlated closely with parameters of depressed myocardial mechanics, the quantitative prevalence of myofibroblasts, and thin fiber collagen deposition, suggesting that treatment with neurohumoral antagonists results in decreased new collagen production. The data obtained in the present study corroborate with information provided by the estimation of collagen synthesis and fragmentation markers in the serum (27–29). Procollagen type III amino-terminal peptide is decreased in chronic heart failure patients using antiangiotensin and anti-aldosterone treatment (30,31).

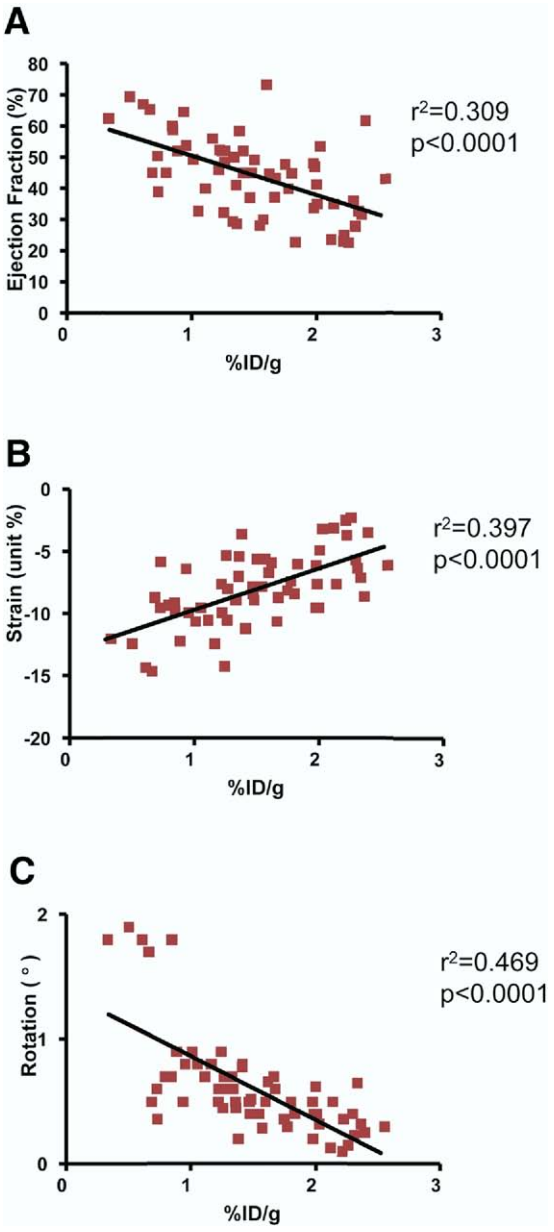

Figure 2. Correlation of Radiolabeled ^{99m}Tc-CRIP Uptake and Echocardiographic Parameters of Remodeling an All Animals

A significant correlation between CRIP uptake and left ventricular ejection fraction (**A**), myocardial strain (**B**), and apical counterclockwise rotation (**C**) is observed. Abbreviations as in Figure 1.

What is the optimum therapy? The clinical role of ACE-I, ARB, and SARA has been conclusively demonstrated in trials confirming the reduction in morbidity and mortality in patients with overt heart failure (8–11,17,32). These agents also decrease the likelihood of the development of heart failure in patients with asymptomatic decrease in LV ejection fraction (13,14), as well as those predisposed to

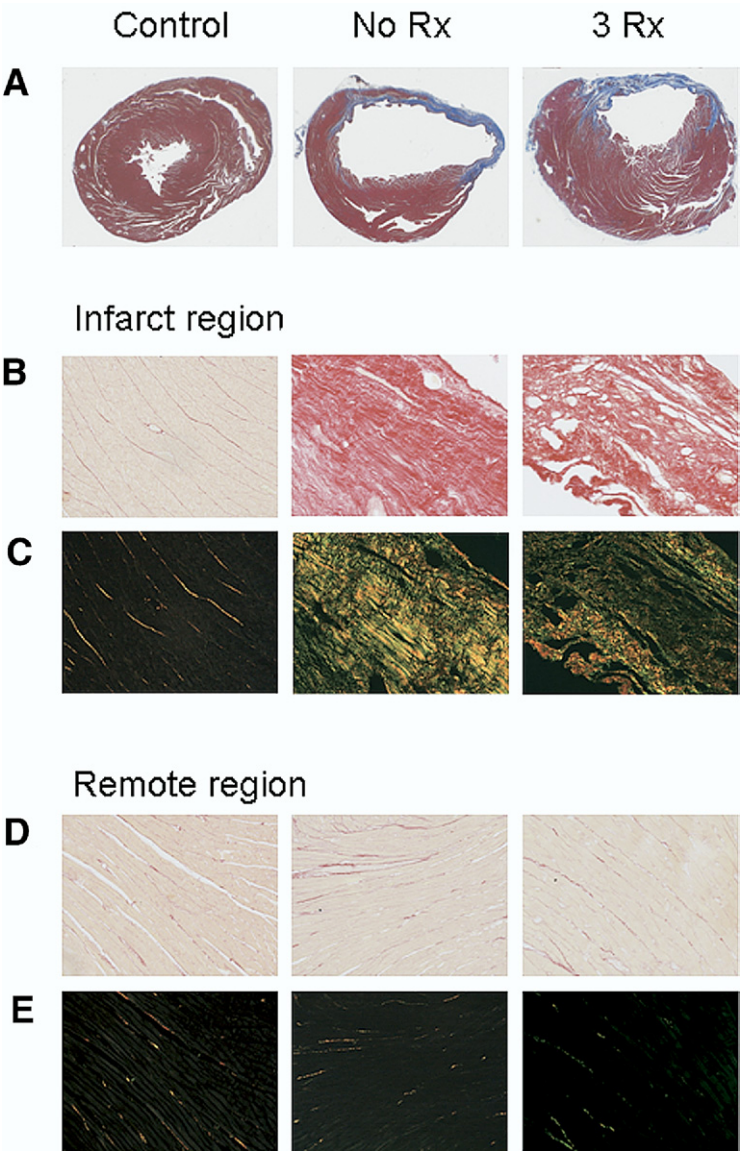

Figure 3. Histopathological Characterization of the Treated and Untreated Animals

Masson's trichrome staining was performed for infarct localization in control, untreated, and treated animals **(A)**. In addition, histological staining was performed with picro Sirius red to demonstrate collagen deposition, which on polarized light allowed identification of the quality of collagen, in the infarct **(B and C)** and remote regions **(D and E)**. The **left column** presents control animals, the **middle column** shows untreated animals (no Rx), and the **right column** shows animals treated with 3Rx neurohumoral antagonists (SCL). The remote region shows minimal fibrosis and collagen deposition **(D)**. On the other hand, infarct region shows significant wall thinning **(A)** and fibrosis with evidence of substantial collagen deposition in untreated animals (**B**, No Rx). 3Rx-treated animals show reduced fibrosis (**A**, SCL) and collagen deposition (**B**, SCL) in the infarcted area. The Sirius staining under polarized light provides distinction of thick red-orange and thin yellow-green collagen fibers in the infarct region **(C)**. SCL = spironolactone, captopril, and losartan.

development of heart failure but normal LV ejection fraction (12,33). It is also established that antiangiotensin agents in combination are superior to any agent used alone. The combination of ACE-I with ARB in the presence of beta-blockers ± aldosterone inhibitors reduces the combined end point of mortality (16) and hospitalization for worsening of heart failure (17). The experimental data from the present study confirm the superior effect of combination of 2 agents. However, the addition of the third agent did not decrease the uptake significantly. It is encouraging to observe the

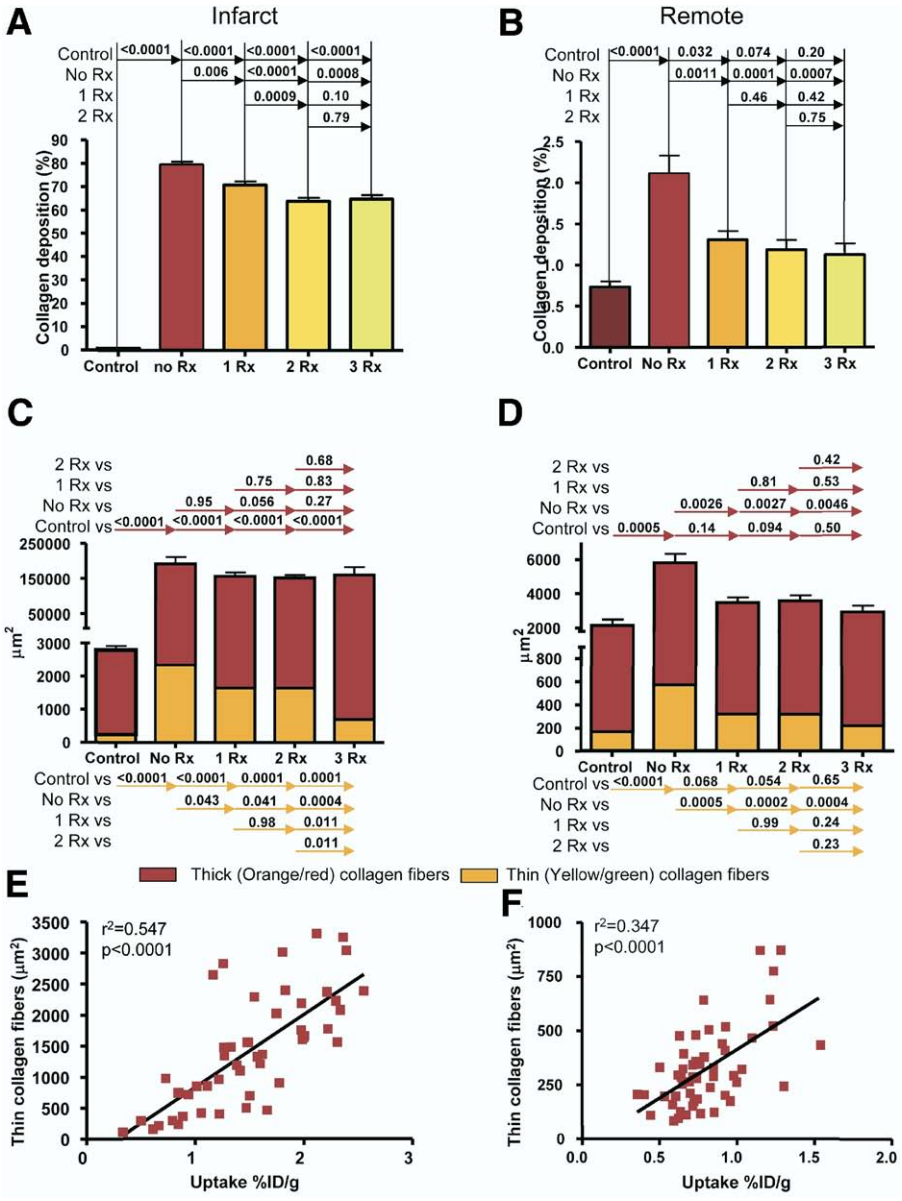

Figure 4. Collagen Fiber Deposition in Infarct and Remote Regions

The total collagen content decreases with treatment in the infarcted **(A)**, as well as the remote **(B)** areas. Further characterization of the collagen fibers by polarization reveals that the thin or new yellow-green collagen fibers decreased both in the infarct **(C)** and remote **(D)** regions after treatment. This indicates cessation of new collagen production and maturation of the collagen fibers after treatment. The prevalence of new collagen fibers paralleled the CRIP uptake and demonstrated a significant direct correlation, both in infarct **(E)** and remote **(F)** regions.

efficacy of an imaging agent to identify difference in infarct healing, which could be of translational clinical benefit.

Is lack of collagen deposition favorable? The present study raises an important question about the relevance of decrease in collagen deposition in the post-infarct patients. Total abolition of collagen deposition, which has been evaluated in clodronate liposome-treated animals (wherein infarct healing becomes defective with minimal collagen deposition and inefficient necrotic myocyte removal) (34), leads to greater tendency for aneurysmal formation and infarct rupture. On the other hand, direct myocardial injection of collagen in experimental infarcts leads to dense collagen deposition and prevents myocardial remodeling (35). Such experi-

Table 3. The Extent of Collagen Deposition and Myofibroblast Count in Various Animal Groups

	Infarct				Remote		
Group	Collagen (%)	YG (mm^2)	OR (mm^2)	ASMA (mm^2)	Collagen (%)	YG (mm^2)	OR (mm^2)
Control	0.90 ± 0.14†	221 ± 79†	2430 ± 402†	0†	0.73 ± 0.18†	170 ± 66†	2052 ± 670†
No Rx	79.3 ± 4.0*	2343 ± 564*	190026 ± 47815*	6.1 ± 5.2*	2.11 ± 0.63*	571 ± 235*	5234 ± 1491*
S	70.9 ± 3.8*†	1452 ± 505	157337 ± 24731*	4.0 ± 2.8	1.32 ± 0.78†	323 ± 268†	3181 ± 1948†
C	71.3 ± 8.2*†	1591 ± 342*	165676 ± 31450*	6.1 ± 2.0*	1.29 ± 0.47†	328 ± 111†	3139 ± 1489†
L	70.1 ± 8.4*†	1849 ± 774*	145112 ± 75498*	4.5 ± 0.5	1.31 ± 0.29†	304 ± 108†	3155 ± 889†
CL	68.2 ± 9.2*†	2304 ± 827*	137198 ± 46884*†	4.2 ± 4.8	1.17 ± 1.04†	298 ± 248†	2950 ± 2678†
SC	61.3 ± 8.5*†	1545 ± 1064*	154679 ± 41481*	1.3 ± 1.4	1.12 ± 0.43†	313 ± 133†	3197 ± 1575†
SL	62.2 ± 7.3*†	1248 ± 937†	168002 ± 27358*	0.7 ± 0.2†	1.32 ± 0.33†	342 ± 79†	3873 ± 1150†
SCL	64.7 ± 3.8*†	689 ± 249†	159914 ± 49453*	1.5 ± 0.9†	1.12 ± 0.41†	291 ± 160†	3321 ± 1499†

*p < 0.05 compared with control animals. †p < 0.05 compared with No Rx-treated animals.
ASMA = alpha smooth muscle cells; OR = orange-red, thick, crosslinked collagen fibers; YG = yellow-green, thin, new collagen fibers; other abbreviations as in Table 2.

ments suggest that the collagen deposition may not necessarily be harmful. However, the use of ACE-I or SARA allows the reduction of collagen deposition as demonstrated by circulating collagen degradation products (30). The present study demonstrated a decrease in collagen deposition with

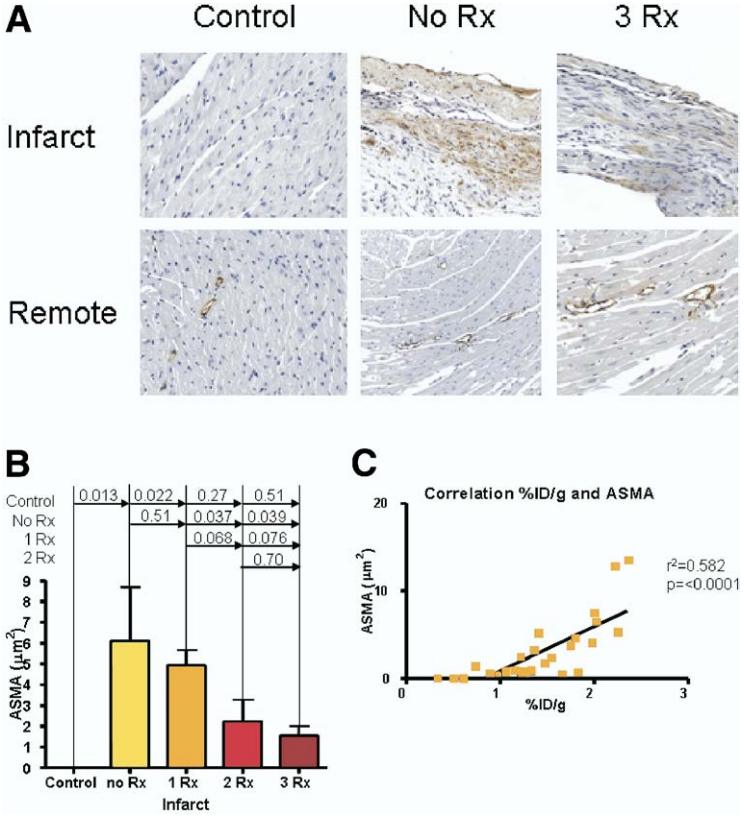

Figure 5. Radiolabeled CRIP Uptake and the Prevalence of ASMA-Verified Myofibroblasts

Immuohistochemical staining with ASMA antibody allowed quantitative assessment of myofibroblasts infiltration in the infarct and remote regions **(A)**. The **left column** presents control animals, the **middle column** shows untreated animals (no Rx), and the **right column** shows 3Rx-animals (SCL). There is a marked decrease in number of myofibroblasts in the infarct region in 2Rx and 3Rx groups **(B)**. There is a significant direct correlation between the extent of myofibroblasts and the CRIP uptake in infarct region **(C)**. ASMA = alpha smooth muscle actin; other abbreviations as in Figures 1 and 3.

suppression of angiotensin-aldosterone axis. Because neurohumoral antagonists lead to favorable clinical outcomes, conceivably reduced collagen deposition should be of benefit. Although the present study is not capable of explaining these paradoxical observations, it is possible that predominant decrease of collagen content observed in the remote myocardium in the present study, and the collagen fiber maturation (to thick fibers) observed in the infarct region may contribute to a more balanced healing.

CONCLUSIONS

The present study demonstrates that ^{99m}Tc-CRIP imaging allows for the evaluation of the efficacy of antiremodeling therapy. It also reconfirms the superiority of combination therapy over a solitary use of neurohumoral antagonists. If proven clinically, molecular imaging of the remodeling processes could facilitate individualizing the treatment for patients susceptible to heart failure.

Acknowledgments

The imaging agents (^{99m}Tc-CRIP and sCRIP) were kindly provided by GE Healthcare, and losartan was a kind gift of Merck & Co.

Reprint requests and correspondence: Dr. Jagat Narula, Division of Cardiology, University of California, Irvine School of Medicine, UCI Main Campus, Medical-Science Building I, Room C 112, Irvine, California 92697. *E-mail: narula@uci.edu.*

REFERENCES

1. Weber KT, Brilla CG. Pathological hypertrophy and cardiac interstitium. Fibrosis and renin-angiotensin-aldosterone system. Circulation 1991; 83:1849–65.
2. Weber KT, Anversa P, Armstrong PW, et al. Remodeling and reparation of the cardiovascular system. J Am Coll Cardiol 1992;20:3–16.
3. Pitt B. Aldosterone blockade in patients with systolic left ventricular dysfunction. Circulation 2003;108: 1790–4.
4. Shirani J, Narula J, Eckelman WC, Narula N, Dilsizian V. Early imaging in heart failure: exploring novel molecular targets. J Nucl Cardiol 2007; 14:100–10.
5. Volders PG, Willems IE, Cleutjens JP, Arends JW, Havenith MG, Daemen MJ. Interstitial collagen is increased in the non-infarcted human myocardium after myocardial infarction. J Mol Cell Cardiol 1993;25: 1317–23.
6. Cleutjens JP, Blankesteijn WM, Daemen MJ, Smits JF. The infarcted myocardium: simply dead tissue, or a lively target for therapeutic interventions. Cardiovasc Res 1999;44: 232–41.
7. Anversa P, Capasso JM. Cardiac hypertrophy and ventricular remodeling. Lab Invest 1991;64:441–5.
8. Pitt B, Poole-Wilson PA, Segal R, et al. Effect of losartan compared with captopril on mortality in patients with symptomatic heart failure: randomised trial—the Losartan Heart Failure Survival Study ELITE II. Lancet 2000; 355:1582–7.
9. The CONSENSUS Trial Study Group. Effects of enalapril on mortality in severe congestive heart failure. Results of the Cooperative North Scandinavian Enalapril Survival Study (CONSENSUS). N Engl J Med 1987;316:1429–35.
10. Cohn JN, Johnson G, Ziesche S, et al. A comparison of enalapril with hydralazine-isosorbide dinitrate in the treatment of chronic congestive heart failure. N Engl J Med 1991;325: 303–10.
11. Pitt B, Zannad F, Remme WJ, et al. The effect of spironolactone on morbidity and mortality in patients with severe heart failure. Randomized Aldactone Evaluation Study Investigators. N Engl J Med 1999;341:709–17.
12. Yusuf S, Sleight P, Pogue J, Bosch J, Davies R, Dagenais G. Effects of an angiotensin-converting-enzyme inhibitor, ramipril, on cardiovascular events in high-risk patients. The Heart Outcomes Prevention Evaluation Study Investigators. N Engl J Med 2000;342:145–53.
13. Pfeffer MA, Braunwald E, Moye LA, et al. Effect of captopril on mortality and morbidity in patients with left ventricular dysfunction after myocardial infarction. Results of the survival and ventricular enlargement trial. The SAVE Investigators. N Engl J Med 1992;327:669–77.
14. Effect of enalapril on survival in patients with reduced left ventricular ejection fractions and congestive heart failure. The SOLVD Investigators. N Engl J Med 1991;325:293–302.
15. Pitt B, Remme W, Zannad F, et al. Eplerenone, a selective aldosterone blocker, in patients with left ventricular dysfunction after myocardial infarction. N Engl J Med 2003;348: 1309–21.
16. Pfeffer MA, Swedberg K, Granger CB, et al. Effects of candesartan on mortality and morbidity in patients with chronic heart failure: the CHARM-Overall programme. Lancet 2003;362: 759–66.
17. Cohn JN, Tognoni G. A randomized trial of the angiotensin-receptor blocker valsartan in chronic heart failure. N Engl J Med 2001;345:1667–75.
18. McNamara DM, Holubkov R, Janosko K, et al. Pharmacogenetic interactions between beta-blocker therapy and the angiotensin-converting enzyme deletion polymorphism in patients with congestive heart failure. Circulation 2001;103:1644–8.
19. Small KM, Wagoner LE, Levin AM, Kardia SL, Liggett SB. Synergistic polymorphisms of beta1- and alpha2C-adrenergic receptors and the risk of congestive heart failure. N Engl J Med 2002;347:1135–42.
20. van den Borne SWM, Isobe S, Verjans J, et al. Molecular imaging of interstitial alterations in remodeling myocardium after myocardial infarction. J Am Coll Cardiol 2008;52: 2017–28.
21. Verjans JWH, Lovhaug D, Narula N, et al. Noninvasive imaging of angiotensin receptores after myocardial infarction. J Am Coll Cardiol Cardiovasc Imaging 2008;1:354–62.
22. Schiller NB, Shah PM, Crawford M, et al. Recommendations for quantitation of the left ventricle by two-dimensional echocardiography. American Society of Echocardiography Committee on Standards, Subcommittee on Quantitation of Two-Dimensional Echocardiograms. J Am Soc Echocardiogr 1989;2:358–67.

JACC: CARDIOVASCULAR IMAGING, VOL. 2, NO. 2, 2009
FEBRUARY 2009:187–98

23. Tonti G, Verjans J, Pedrizzetti G, et al. Measurement of apical torsion in mitochrondrial cardiomyopathy using a novel B-mode, automated tracking algorithm. J Am Coll Cardiol 2005; 45:305A.
24. Whittaker P, Kloner RA, Boughner DR, Pickering JG. Quantitative assessment of myocardial collagen with picrosirius red staining and circularly polarized light. Basic Res Cardiol 1994;89:397–410.
25. MacKenna DA, Omens JH, McCulloch AD, Covell JW. Contribution of collagen matrix to passive left ventricular mechanics in isolated rat hearts. Am J Physiol 1994;266: H1007–18.
26. Verjans JW, Wolters SL, Lax M, et al. Imaging avb3/b5 Integrin Upregulation in Patients After Myocardial Infarction. Circulation 2007; 116:II3288.
27. Poulsen SH, Host NB, Jensen SE, Egstrup K. Relationship between serum amino-terminal propeptide of type III procollagen and changes of left ventricular function after acute myocardial infarction. Circulation 2000;101:1527–32.
28. Cicoira M, Rossi A, Bonapace S, et al. Independent and additional prognostic value of aminoterminal propeptide of type III procollagen circulating levels in patients with chronic heart failure. J Card Fail 2004;10:403–11.
29. Radovan J, Vaclav P, Petr W, et al. Changes of collagen metabolism predict the left ventricular remodeling after myocardial infarction. Mol Cell Biochem 2006;293:71–8.
30. Zannad F, Alla F, Dousset B, Perez A, Pitt B. Limitation of excessive extracellular matrix turnover may contribute to survival benefit of spironolactone therapy in patients with congestive heart failure: insights from the randomized aldactone evaluation study (RALES). Rales Investigators. Circulation 2000;102:2700–6.
31. Zannad F, Radauceanu A. Effect of MR blockade on collagen formation and cardiovascular disease with a specific emphasis on heart failure. Heart Fail Rev 2005;10:71–8.
32. McMurray JJ, Ostergren J, Swedberg K, et al. Effects of candesartan in patients with chronic heart failure and reduced left-ventricular systolic function taking angiotensin-converting-enzyme inhibitors: the CHARM-Added trial. Lancet 2003;362:767–71.
33. Yusuf S, Teo KK, Pogue J, et al. Telmisartan, ramipril, or both in patients at high risk for vascular events. N Engl J Med 2008;358:1547–59.
34. van Amerongen MJ, Harmsen MC, van Rooijen N, Petersen AH, van Luyn MJ. Macrophage depletion impairs wound healing and increases left ventricular remodeling after myocardial injury in mice. Am J Pathol 2007; 170:818–29.
35. Dai W, Wold LE, Dow JS, Kloner RA. Thickening of the infarcted wall by collagen injection improves left ventricular function in rats: a novel approach to preserve cardiac function after myocardial infarction. J Am Coll Cardiol 2005;46:714–9.

Key Words: collagen ■ remodeling ■ radionuclide imaging ■ angiotensin receptors ■ angiotensin-converting enzyme ■ mineralocorticoids ■ heart failure.